Interactions of solitons with a Gaussian barrier: splitting and recombination in quasi-one-dimensional and three-dimensional settings

2013 New J. Phys. 15 063006

(http://iopscience.iop.org/1367-2630/15/6/063006)

New Journal of Physics
The open access journal for physics

Interactions of solitons with a Gaussian barrier: splitting and recombination in quasi-one-dimensional and three-dimensional settings

J Cuevas[1,5], P G Kevrekidis[2], B A Malomed[3], P Dyke[4] and R G Hulet[4]

[1] Grupo de Física No Lineal, Departamento de Física Aplicada I, Universidad de Sevilla, Escuela Politénica Superior, C/ Virgen de Africa, 7, E-41011 Sevilla, Spain
[2] Department of Mathematics and Statistics, University of Massachusetts, Amherst, MA 01003-4515, USA
[3] Department of Physical Electronics, School of Electrical Engineering, Faculty of Engineering, Tel Aviv University, Tel Aviv 69978, Israel
[4] Department of Physics and Astronomy, Rice University, Houston, TX 77005, USA
E-mail: jcuevas@us.es

New Journal of Physics **15** (2013) 063006 (16pp)
Received 16 January 2013
Published 6 June 2013
Online at http://www.njp.org/
doi:10.1088/1367-2630/15/6/063006

Abstract. The interaction of matter–wave solitons with a potential barrier is a fundamentally important problem, and the splitting and subsequent recombination of the soliton by the barrier is the essence of soliton matter–wave interferometry. We demonstrate the three-dimensional (3D) character of the interactions in the case relevant to ongoing experiments, where the number of atoms in the soliton is relatively close to the collapse threshold. We examine the soliton dynamics in the framework of the effectively one-dimensional (1D) nonpolynomial Schrödinger equation (NPSE), which admits the collapse in a modified form, and in parallel we use the full 3D Gross–Pitaevskii equation (GPE). Both approaches produce similar results, which are, however, quite

[5] Author to whom any correspondence should be addressed.

different from those produced in recent work that used the 1D cubic GPE. Basic features, produced by the NPSE and the 3D GPE alike, include (a) an increase in the first reflection coefficient for increasing barrier height and decreasing atom number; (b) large variation of the secondary reflection/recombination probability versus barrier height; (c) pronounced asymmetry in the oscillation amplitudes of the transmitted and reflected fragments; and (d) enhancement of the transverse excitations as the number of atoms is increased. We also explore effects produced by variations of the barrier width and outcomes of the secondary collision upon phase imprinting on the fragment in one arm of the interferometer.

Contents

1. Introduction

Ongoing studies of atomic Bose–Einstein condensates (BECs) have contributed numerous fundamental insights in a wide range of phenomena [1, 2]. This may be largely attributed to the precise control afforded by experiments, and to the existence of accurate, yet quite tractable models based on the Gross–Pitaevskii equation (GPE) [3, 4]. Many of the theoretical and experimental investigations have strong connections to other areas, such as condensed matter physics, nonlinear optics, superconductivity and superfluidity. Furthermore, ultracold gases trapped in external potentials may be utilized as quantum simulators of real materials [5].

Inter-atomic interactions in a BEC enable the examination of a wide variety of nonlinear effects that have been summarized in a number of reviews and books such as [4]. Basic types of coherent structures built by the nonlinearity are bright solitons and soliton complexes [6–10], dark solitons [11], vortices and vortex lattices [12–15]. Bright solitons were proposed for matter–wave interferometry [16], which is itself an active field of research [17]. Recent work has focused on the role of the condensate's effective nonlinearity [18] as well as on advanced applications [19]. Solitons may provide 100-fold improved sensitivity for atom interferometry, where their long lifetime, of the order of seconds, may enable precise force sensing [20] and measurement of small magnetic field gradients [21]. Robust bright solitons, appropriate for these applications, have been created under well-controlled conditions in BECs with attractive [16, 22, 23] and repulsive [24] inter-atomic interactions (in the latter case, these were gap solitons [7] supported by the optical-lattice potential). A topic of particular interest has been the splitting and subsequent recombination of solitons due to collisions with potential barriers. This was studied theoretically in detail [25–28], as summarized in a recent review [29].

However, it is relevant to stress that the analysis has been thus far carried out for a one-dimensional (1D) model, i.e. the 1D GPE with cubic nonlinearity (although some features such as solitary-wave collisions have also been recently explored in a three-dimensional (3D) setting [30]). In the same framework, the quasiparticle–wave duality of solitons and their tunneling through a potential barrier have been recently considered [32, 33].

The subject of this work is the interaction of the incident soliton with a potential barrier, acting as a beam splitter, and the subsequent recombination of the split fragments in the 3D setting. The three-dimensionality strongly affects the results in comparison with the 1D setting adopted in the above-mentioned recent studies. Bright matter–wave solitons are experimentally created in cigar-shaped (nearly 1D) potential traps in which the self-trapping is driven by intrinsic attractive nonlinearity solely in the axial direction. The number of atoms in the soliton, N, will be considered to be relatively close to the value at the collapse threshold, N_c, and the actual shape of the solitons will be three-dimensional in the considerations that follow. Accordingly, the solitary waves do not reproduce the conspicuous elongation of the underlying trapping potential, as known from previous studies [6, 16, 22, 23]. Thus, the character of the splitting and subsequent merger may be essentially three-dimensional too—in particular, transverse modes may (and will, as we show) be excited.

In the recently studied 1D counterpart of this setting, the results of an earlier study [34] were used in [26] to predict the transmission and reflection coefficients and the phase shift resulting from the interaction with a narrow barrier. A sinusoidal dependence of the transmission coefficient on the relative phase of two solitary waves colliding on the barrier was identified. In [27], both the primary splitting of a single solitary wave and the secondary collision of the two fragments were studied using the truncated Wigner approximation, with emphasis on the comparison of the mean-field dynamics with the quantum dynamics. Significant deviations between the two were identified for a relatively small number of atoms in the solitary wave. A stepwise (discontinuous) variation of the reflection and transmission coefficients due to quantum superposition has been recently reported [28, 31, 32]. The deviation between the quantum and mean-field approaches is significant only for relatively small N, becoming negligible for large N. In this paper, we consider N close to collapse, where $N_c \simeq 10^5$. For this reason, quantum effects are not crucially important to us.

Collisions of 1D solitons with an attractive potential well, rather than the repulsive barrier, have also been studied recently, revealing a fairly complex phenomenology. The latter features alternating windows of transmission, reflection and trapping with abrupt transitions between them as the potential depth varies [35, 36].

Our analysis is performed in two stages. Firstly, we use the well-known 1D nonpolynomial Schrödinger equation (NPSE) [37, 38], which, unlike the cubic 1D GPE, captures the 3D phenomenology in some approximation (in particular, it admits the possibility of collapse, although not in the same way as the 3D GPE). We will refer to this NPSE setting as a quasi-1D description to clearly distinguish it from the 1D GPE setting where collapse is absent. Secondly, we report the results obtained from the full 3D GPE. To the best of our knowledge, both equations are used for the first time in this context. Our main interest is to consider relatively large atom numbers N ($N = 80\,000 \simeq 0.85N_c$), for which the phase coherence of the condensate is maintained and the soliton dynamics are most interesting. We explore the dependence of the results on N, as well as on the height of the barrier, E. There exist significant differences between the dynamics described by the ordinary cubic 1D GPE and predictions of the full 3D equation, as the excitation of transverse oscillations (the feature that is obviously absent in the

1D description) becomes prominent for $N \to N_c$. On the other hand, the quasi-1D NPSE is found to be in reasonable agreement with the 3D GPE in regard to both its static properties (although the stable branch of solutions at low N is captured more accurately than the unstable collapsing one of high N) and the dynamics of soliton–barrier interactions.

The paper is structured as follows. In section 2, we introduce the quasi-1D and 3D models, compute their stationary solutions and define the diagnostics used to examine the dynamics. In section 3, we report numerical results in detail, varying the barrier height and width, atom number as well as phase imprinting applied to one of the fragments for simulating the interferometry. Section 4 concludes the paper.

2. Model equations and stationary solutions

We start by introducing the quasi-1D NPSE for the mean-field wave function, ψ, of the condensate of ^{7}Li atoms loaded into a cigar-shaped trap with axial coordinate z,

$$i\hbar \frac{\partial \psi}{\partial t} = -\frac{\hbar^2}{2m}\frac{\partial^2 \psi}{\partial z^2} + V(z)\psi + \frac{1 + (3/2)g|\psi|^2}{\sqrt{1 + g|\psi|^2}}\psi, \tag{1}$$

where $g = 2a_s/a_\perp$, with the typical scattering length $a_s = -0.3a_0$, where a_0 is the Bohr radius, and transverse trapping radius $a_\perp = \sqrt{\hbar/(m\omega_\perp)} = 2.25\,\mu$m, which corresponds to a confinement frequency $\omega_\perp = 2\pi\,290$ Hz and atomic mass $m = 7$ amu. The longitudinal potential $V(z)$ includes a weak parabolic trap, which we assume has a typical value of the strength, $\omega_z = 2\pi\,5.6$ Hz, and the Gaussian barrier of height E and width ε, which will be varied below:

$$V(z) = (1/2)m\omega_z^2 z^2 + E\exp(-2z^2/\varepsilon^2). \tag{2}$$

The total number of atoms, given by $N = \int_{-\infty}^{+\infty} dz\,|\psi(z)|^2$, will also be varied.

The results produced by the NPSE (1) will be compared with those obtained from the radially symmetric 3D GPE, written in cylindrical coordinates (ρ, z) as

$$i\hbar \frac{\partial \psi}{\partial t} = -\frac{\hbar^2}{2m}\left(\frac{\partial^2 \psi}{\partial \rho^2} + \frac{1}{\rho}\frac{\partial \psi}{\partial \rho} + \frac{\partial^2 \psi}{\partial z^2}\right) + V(\rho, z)\psi + \frac{4\pi\hbar^2}{m}a_s|\psi|^2\psi \tag{3}$$

with $N = 2\pi\int_0^\infty \rho\,d\rho\int_{-\infty}^{+\infty} dz\,|\psi(\rho, z)|^2$ and the 3D potential

$$V(\rho, z) = (1/2)m(\omega_\perp \rho^2 + \omega_z^2 z^2) + E\exp(-2z^2/\varepsilon^2). \tag{4}$$

Equation (4) implies that we consider only fundamental axially symmetric solitons, but not ones with intrinsic axial vorticity, which are also possible in this setting [38]. Axial widths of the solitons generated by the quasi-1D NPSE and 3D GPE are defined as

$$W_{1D} = 2\sqrt{N^{-1}\int_{-\infty}^{+\infty} dz\,z^2|\psi|^2}, \quad W_{3D} = 2\sqrt{N^{-1}\int_0^\infty \rho\,d\rho\int_{-\infty}^{+\infty} dz\,z^2|\psi|^2}. \tag{5}$$

Stationary solutions with chemical potential μ were sought as $\psi(\mathbf{r}, t) = \exp(-i\mu t/\hbar)\psi(\mathbf{r})$. Figure 1 compares the $N(\mu)$ and $W(N)$ curves for soliton families, produced by both the quasi-1D and 3D equations. In these plots, N is normalized to the critical atom number, N_c, which initializes the collapse, i.e. the largest number of atoms accessible (in terms of stable solitons) in the given setting [39, 40]. Both equations yield nearly the same value, $N_c \approx 94\,000$. The same plot includes the curves for the usual 1D cubic GPE,

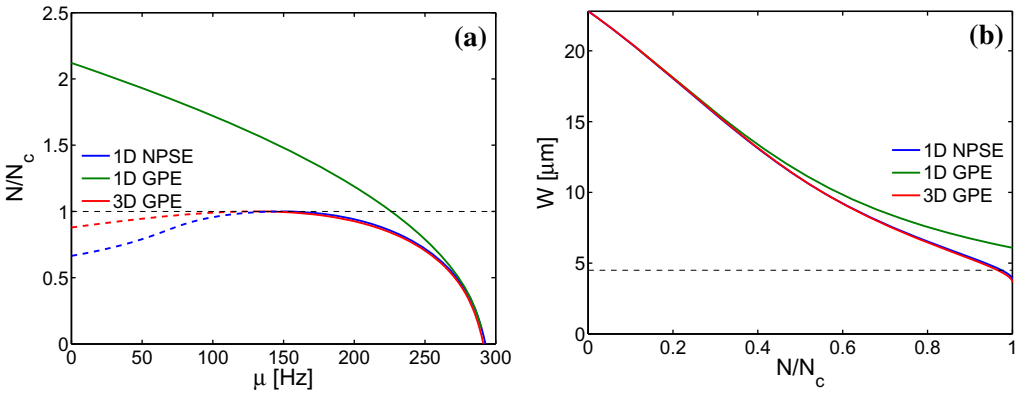

Figure 1. (a) The number of atoms, normalized to its critical value at the collapse threshold, N/N_c, versus the chemical potential, for the stable ($\mu > \mu_c$) and unstable ($\mu < \mu_c$) soliton families; $\mu_c = 147.9$ Hz for the quasi-1D NPSE (1), and $\mu_c = 130.5$ Hz for the 3D GPE (3). (b) The axial widths, defined as per (5), versus N/N_c, for the stable soliton family. The dark dashed horizontal curve in the right panel corresponds to the width of 4.5 μm, which is a typical width of the barrier in what follows. The reference value of chemical potential μ for vanishing interaction is given by the transverse oscillator frequency, here $\omega_\perp/(2\pi) = 290$ Hz. The limit value of the width for the vanishing interaction strength is the confinement length of the longitudinal trapping potential, $W = \sqrt{2\hbar/m\omega_z} = 22.8\,\mu$m. Both panels also display the comparison with the results produced by the usual 1D cubic GPE; as expected, that equation is only able to reproduce results for a relatively small number of atoms, $N \lesssim 0.5N_c$.

demonstrating that the latter model progressively deviates from the NPSE and the 3D GPE for $N/N_c \gtrsim 0.5$. It is relevant to note that the solitons of the former model have a monotonic dependence of N on μ corroborating their dynamical stability for all values of the chemical potential, contrary to the instability of the latter two models for $N > N_c$. It is for these reasons that for the range of atom numbers examined herein, we will restrict our considerations to the latter two models. The change of the soliton properties with the increase of N also illustrates the crossover from the nearly 1D to nearly 3D situations in the present setting.

A straightforward analysis demonstrates that the general condition for the validity of the NPSE approximation is $N/N_c \simeq N|a|/a_\perp < 1$. Indeed, it is observed in figure 1 that stable solution branches generated by the NPSE and 3D GPE are very close, while the discrepancy is conspicuous for unstable branches. In the right panel of figure 1, a horizontal line is drawn at $W = 4.5\,\mu$m, which corresponds to the typical width of the barrier ε in the simulations reported below. It is seen that stable solitons are narrower than 4.5 μm only at $N > 0.98N_c$. Consequently, solitons are typically wider than the considered barrier.

In what follows, we will keep the trap strength fixed and will vary the number of atoms N. We will be interested in the regime of large N (and close to the onset of collapse), where the mean-field approximation is expected to adequately describe the system. In contrast, for cases of tighter confinement or of lower atom numbers, the effects of quantum fluctuations are expected to progressively become more important [27].

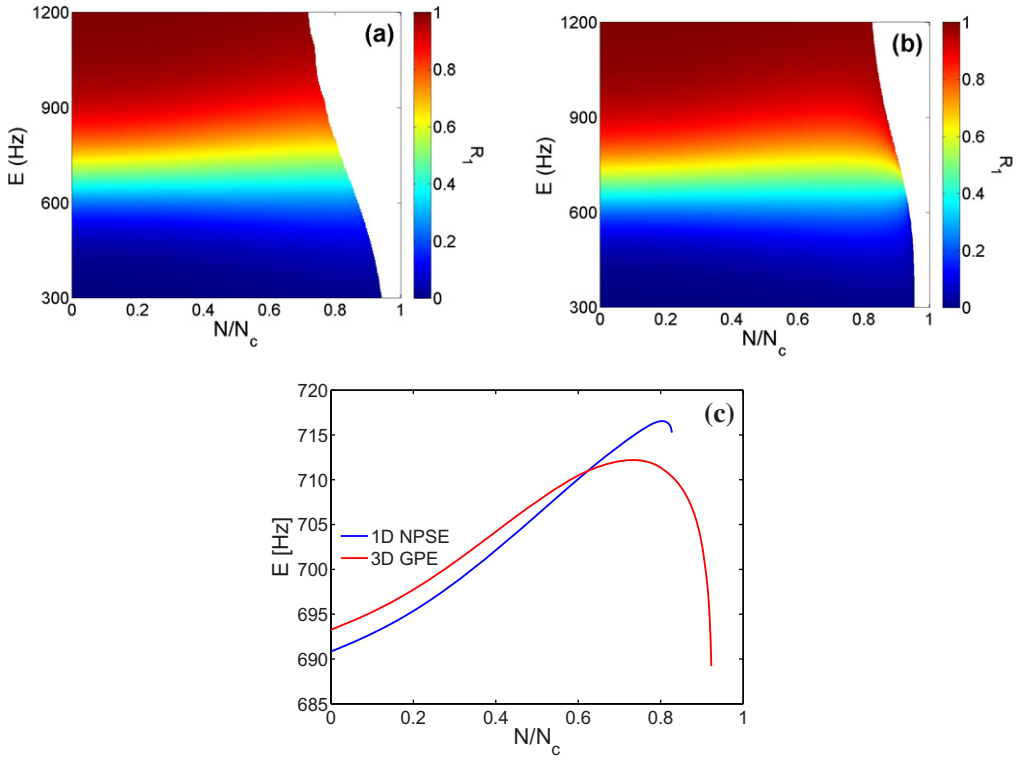

Figure 2. The first reflection coefficient, R_1 (see (6)), versus barrier height, E, and the normalized number of atoms, N/N_c, in the quasi-1D (a) and 3D (b) settings. Blank regions correspond to barrier-induced collapse. Panel (c) shows the value of the barrier height at which equal splitting ($R_1 = 0.5$) is attained, as a function of N/N_c. The barrier width is $\varepsilon = 4.5\,\mu$m.

3. Numerical simulations

3.1. Effect of changing the number of atoms

We first consider simulations for the solitons launched with zero velocity at the distance $A = 251\,\mu$m from the central position where the barrier is placed. In the present setting, this amounts to the initial potential energy equal to 678 Hz. The barrier is here taken with a fixed width, $\varepsilon = 4.5\,\mu$m. The number of atoms in the soliton and the barrier height E are varied and the outcome of the soliton–barrier interaction is monitored. The splitting is characterized by the time-dependent reflection coefficient,

$$R_{1D}(t) = N^{-1}\int_{-\infty}^{0} dz\,|\psi|^2, \quad R_{3D}(t) = N^{-1}\int_0^{\infty}\rho\,d\rho\int_{-\infty}^{0} dz\,|\psi|^2, \tag{6}$$

which shows the fraction of atoms remaining in the incident arm of the interferometer. Below, we focus on R taken at two specific times, $R_1 \equiv R(t = \pi/\omega_z)$ and $R_2 \equiv R(t = 2\pi/\omega_z)$. The former value measures the fraction of atoms that remain in the original arm after the interaction of the incoming soliton with the barrier, because $t = \pi/\omega_z$ corresponds to a half-period of oscillation of the soliton in the weak longitudinal trap, thus ensuring that its first collision with the barrier (occurring roughly at a quarter of the period) is completed. The latter value, R_2,

measures the relevant fraction after the second interaction, i.e. the collision of the returning fragments with the potential barrier. This occurs at roughly three quarters of the oscillation period, while R_2 is measured at a full period (defined in the absence of the barrier).

Figures 2 and 3 show, respectively, R_1 and R_2 versus the number of atoms, N, and the barrier height, E, with the blank regions denoting the presence of collapse. Collapse occurs for $N < N_c$ in these cases due to interaction with the barrier. It is observed that the quasi-1D NPSE and 3D GPE dynamics show similar trends for the first reflection. Namely, the reflection increases with the growth of the barrier height and with decreasing N. The second reflection coefficient, R_2, presents a more complex functional dependence, which, in terms of the quasi-1D NPSE and 3D GPE alike, features an oscillatory variation with N and E for sufficiently large N. Nevertheless, we observe good qualitative and even semi-quantitative agreement between the quasi-1D and the fully 3D models in this context. This behavior can be attributed to the number-dependent variation of phases and amplitudes of the fragments emerging from the first collision, which, upon their recombination, leads to outcomes ranging from the nearly perfect reflection of the recombined soliton to its nearly perfect transmission. This is a more complex manifestation of the feature observed in [26] and is a nonlinear effect stemming from the interference of the phases of the two fragments, becoming progressively more pronounced as $N \to N_c$. This phenomenon is especially visible for $N/N_c \gtrsim 0.3$, leading to a series of resonant peaks of full reflection. Another interesting feature is the presence of finger-like gaps in the quasi-1D setting where collapse occurs after the second interaction with the barrier, when $N/N_c \gtrsim 0.85$. Those gaps do not appear in the 3D setting (not shown here in detail), indicating that they originate from an inherent limitation of the NPSE approximation. This is explained by the fact that in the framework of the NPSE (1) the soliton collapses when the denominator vanishes, at the critical value of the peak density (contrary to the genuine collapse of the fully 3D setting). This difference also explains the apparently wider range of parameters (in the $(E, N/N_c)$ parametric plane) leading to collapse for the quasi-1D problem in comparison to the fully 3D one. Finally, the right panel of figure 3 shows the increase in the second reflection with increasing N, for the case in which E is adjusted to give 50% splitting after the first reflection.

While the reflectivity provides a measure of the asymmetries between the atom-number fractions emerging to the left and right of the barrier, we have used additional diagnostics to quantify the dynamics. In particular, as a measure of the asymmetry of the reflected and transmitted waveforms, we define

$$\zeta \equiv \frac{A_t - A_r}{A_t + A_r}, \tag{7}$$

where A_r and A_t are the oscillation amplitudes within the trap of the reflected and transmitted fragments, and both are taken to be positive. The dependence of ζ on N/N_c and E is presented in figure 4, along with its dependence on N/N_c when E is adjusted to give 50% splitting. An interesting feature is that $\zeta > 0$ for every N and E, i.e. the transmitted fragment always reaches a higher value of $|z|$ and, consequently, has a higher kinetic energy, independently of whether it is the larger or smaller fragment. This can presumably be attributed to the original direction of motion (and associated momentum) of the incoming solitary wave. It should also be noted that typically the most pronounced asymmetries occur for larger values of N/N_c, appearing to be predominantly a feature of the 3D nature of the interactions in that case.

To assess the impact of the width of the barrier on the above results, we have performed a complementary study for the 1D NPSE, considering a narrower barrier whose width is

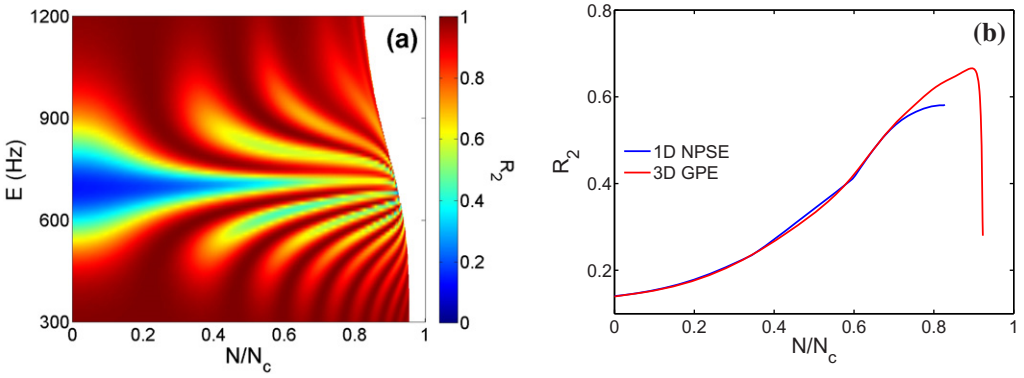

Figure 3. Panel (a) shows the second reflection coefficient, R_2 (see (6)), versus the barrier height, E, and the normalized number of atoms, N/N_c, in the 3D setting. The barrier-induced collapse occurs in blank areas. Panel (b) shows the typically increasing trend of R_2 as a function of N/N_c when $R_1 = 0.5$. The barrier width is $\varepsilon = 4.5\,\mu$m.

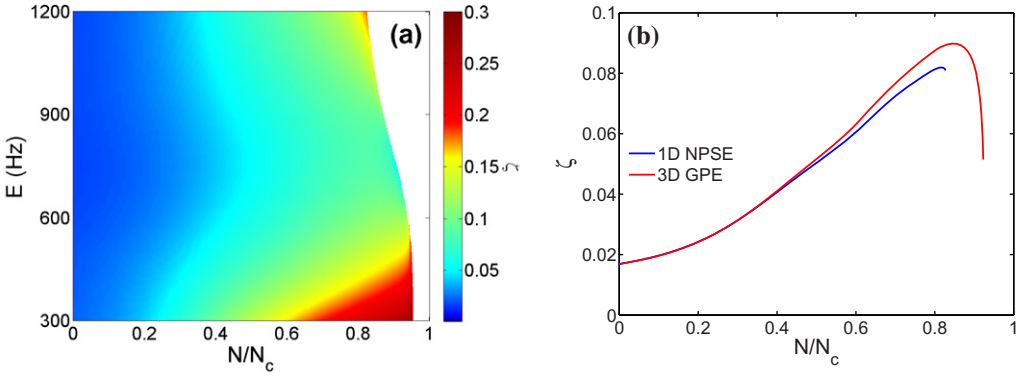

Figure 4. (a) Oscillation asymmetry, ζ (see the definition of (7)), after the first barrier interaction as a function of E and N/N_c, in the 3D setting (as with previous panels, the contour plot is essentially identical for the quasi-1D case of the NPSE). (b) ζ versus N/N_c when $R_1 = 0.5$. The barrier width is $\varepsilon = 4.5\,\mu$m.

$\varepsilon = 1\,\mu$m, a value much less than the axial width of the soliton. Figure 5 shows the dependence of R_1 (a), R_2 (b) and ζ (c) with respect to N and E as before. The qualitative nature of the dependence of these quantities does not seem to change in comparison to the case of $\varepsilon = 4.5\,\mu$m. Nevertheless, there is a quantitative shift of the principal features toward higher values of the barrier height E, as expected.

A basic feature of the 3D dynamics, which may be naturally expected, and is indeed produced by the 3D GPE, is the excitation of radial oscillations after splitting. This feature is, by construction, not incorporated in the 1D GPE, where the transverse shape is assumed to be 'frozen'. On the other hand, it is incorporated in a simple (yet reasonably accurate) way in the quasi-1D description of the NPSE, through the assumption of a space- and time-dependent width of the transverse direction of the ground state that is directly controlled (according to the Euler–Lagrange equations) by the longitudinal wave function. This feature is partially responsible for the good agreement between the quasi-1D NPSE and the fully 3D GPE, as

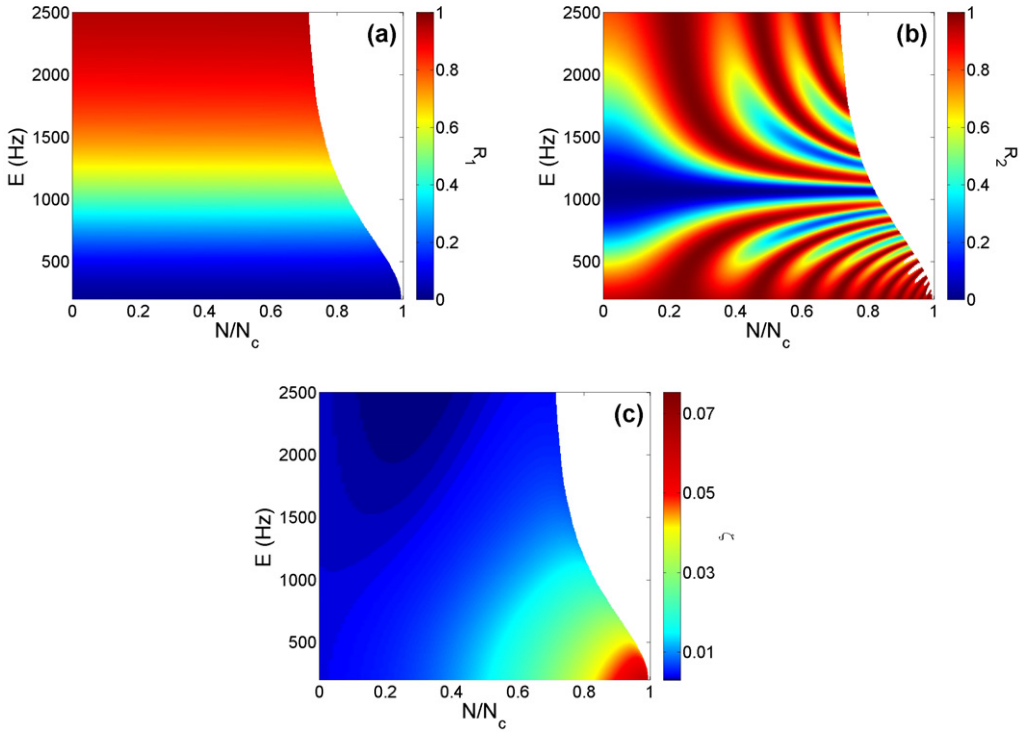

Figure 5. First reflection coefficient R_1 (a), second reflection coefficient R_2 (b), and the oscillation asymmetry ζ (c) versus E and N/N_c, in the quasi-1D setting of the NPSE when $\varepsilon = 1\,\mu$m.

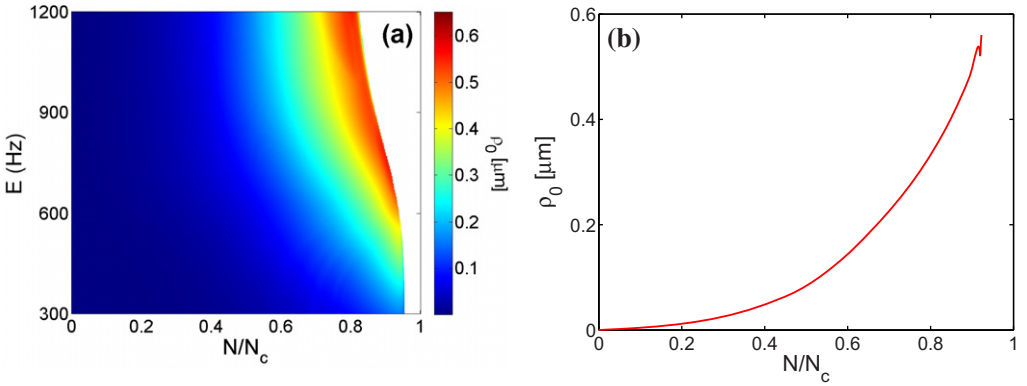

Figure 6. (a) Amplitude ρ_0 of radial oscillations in the 3D setting excited by the first interaction with the barrier, as a function of E and N/N_c. In (b), the value of ρ_0 is plotted versus N/N_c, while $R_1 = 0.5$ is fixed. The barrier width is $\varepsilon = 4.5\,\mu$m.

observed above. We quantify the radial vibrations in the 3D case by evaluating a measure of their amplitude

$$\bar{\rho}(t) = \frac{2\pi}{N} \int_0^{\infty} \rho \, \mathrm{d}\rho \int_{-\infty}^{+\infty} \mathrm{d}z \, \rho |\psi|^2, \tag{8}$$

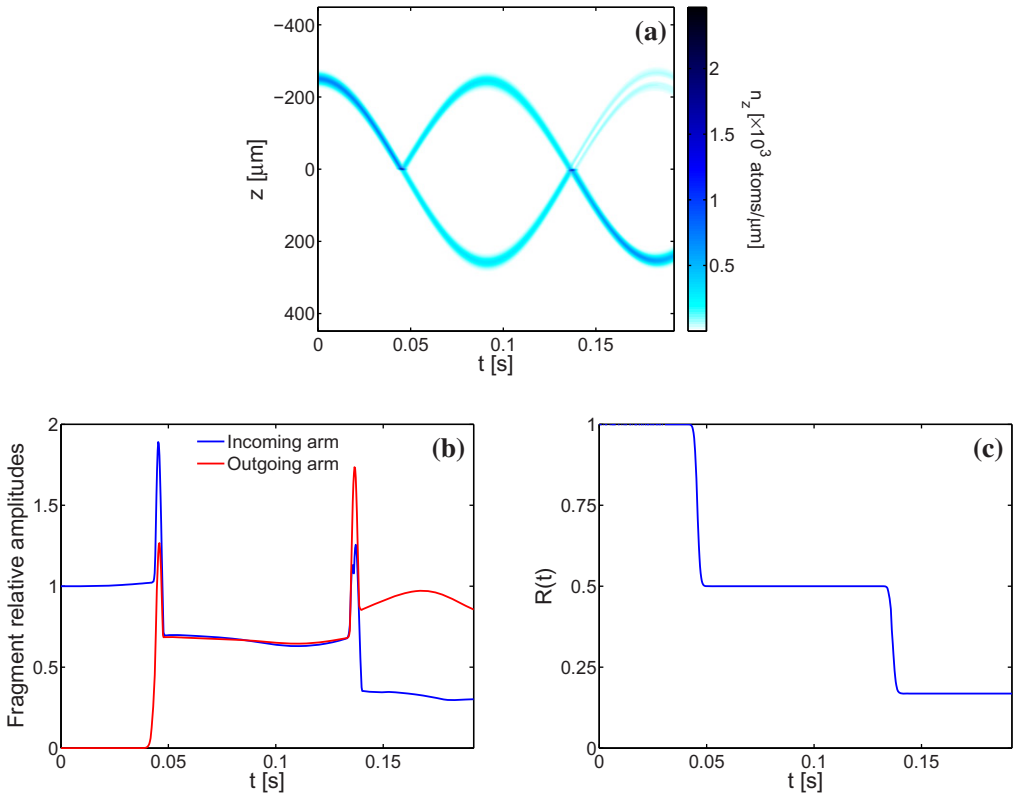

Figure 7. Interaction with a barrier of width $\varepsilon = 4.5\,\mu$m giving $R_1 = 0.5$ and small R_2 (i.e. even splitting of the incident soliton followed by the recombination of fragments into a nearly single transmitted one) in the 3D GPE (3). (a) Integrated density plots. (b) Amplitudes of the fragments divided by amplitude of the initial soliton (c) Time-dependent reflection coefficient. The present results were obtained with $N \approx 0.17 N_c$ and $E = 696.95$ Hz. The smallest value of the second reflection coefficient is $R_2 = 0.17$. The outcome for the quasi-1D NPSE is essentially similar.

and defining ρ_0 as the maximum value of $\bar{\rho}$ (over time for a given set of parameters). Figure 6(a) shows the dependence of ρ_0 on N/N_c and E, together with its value at the barrier height E_{sp} corresponding to $R_1 = 0.5$ (b). It is clearly observed that with the increase of N/N_c and E, the excitation of transverse oscillations becomes very significant, with the amplitude attaining values $\simeq 0.5\,\mu$m. The same conclusions are suggested by the right panel for the case of even splitting. Hence, it can be inferred that the role of higher dimensionality (captured qualitatively within our quasi-1D NPSE approach and properly incorporated in the fully 3D setting) is of particular relevance for N close to N_c (a case of central interest to ongoing experiments).

Figures 7 and 8 show the outcomes of simulations corresponding, respectively, to small and large values of R_2, in the 3D setting (results for the quasi-1D NPSE are quantitatively similar). The figures display longitudinal (z-dependent) density, resulting from the integration of the density in the transverse plane (denoted as n_z), along with amplitudes of the fragments and the time-dependent reflection coefficients, which exhibit jumps upon the interaction of one

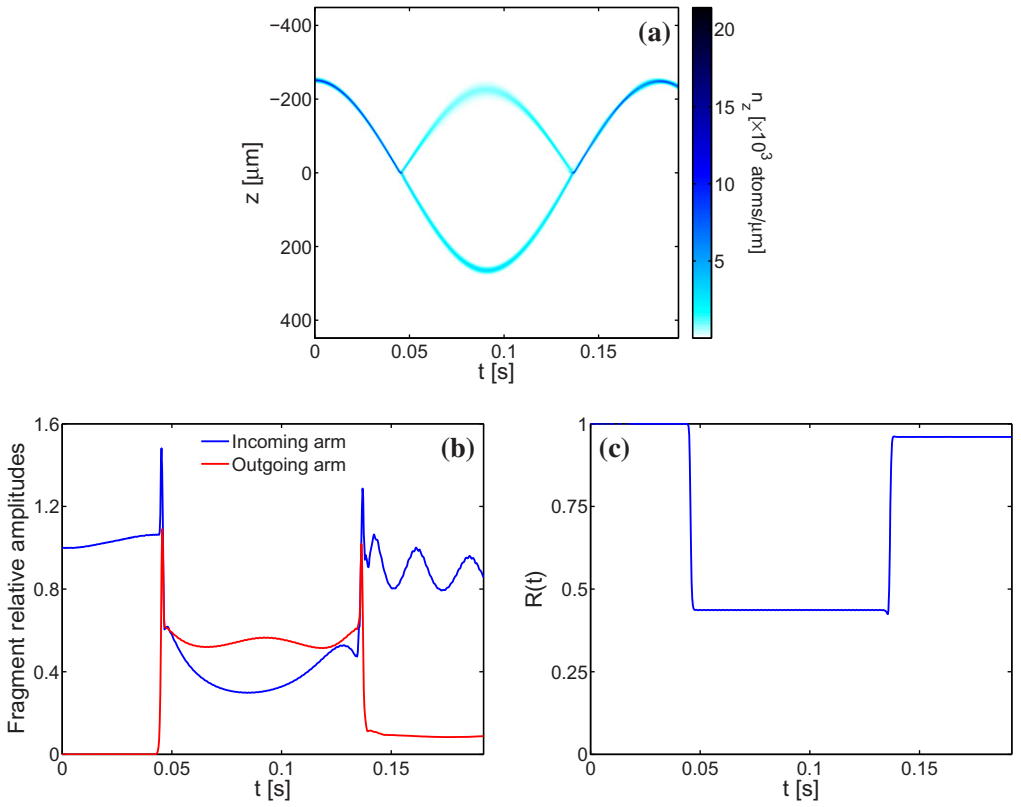

Figure 8. As in figure 7, but for the case of R_2 close to 1, i.e. the recombined soliton returning in the incoming arm. $N \approx 0.88N_c$ and $E = 686$ Hz, resulting in $R_1 = 0.44$ and $R_2 = 0.96$.

(during the first event) or of two (during the second event) solitary wave(s) with the barrier. As these figures show, the amplitudes of the fragments can be different even when the numbers of atoms in them are equal. Naturally, the width is larger for the fragment with the lower peak density. Furthermore, in addition to the two limiting cases, our results suggest that one can manipulate the parameters (such as E, N, etc) controlling the interaction of the incident soliton with the barrier to produce any desired outcome within a wide range in the sequence of two collisions. While there appear to be two waves in figure 7 for $z < 0$, after the second soliton–barrier interaction, this feature can be controlled (and avoided) through the use of a narrower barrier (results not shown here).

3.2. Effect of changing the initial position of the soliton

In this subsection the number of atoms is fixed to $N = 0.8N_c$, which is a typical, experimentally reachable value where the 3D nature of the condensate is crucial to the observed dynamics. Hence, we expect the 3D GPE to be a suitable model, and the quasi-1D NPSE to be a good qualitative (and reasonable quantitative) approximation. We also expect transverse excitations to be present in the dynamics.

We display here the dependence on initial displacement A from which the soliton is launched with zero velocity (a parameter that effectively characterizes the kinetic energy of

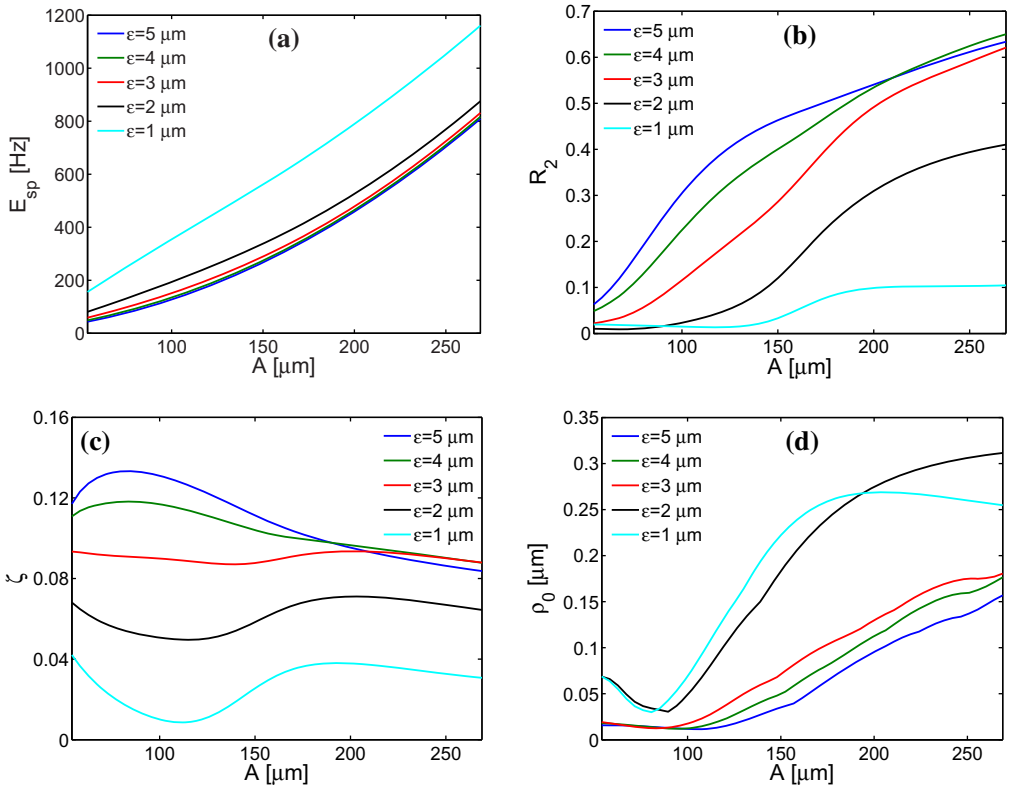

Figure 9. Dependences of characteristics of the interaction on the initial displacement of the incident soliton, A, for $N = 0.8N_c$. (a) The barrier height, E_{sp}, necessary for 50% splitting after the first collision. In the following plots, $E = E_{sp}$: (b) secondary reflection coefficient, R_2; (c) asymmetry coefficient ζ, defined as per (7); and (d) amplitude of the radial oscillations, ρ_0. The displayed results are produced by the 3D GPE (3).

the incident soliton). For the sake of completeness, we do this for different barrier widths in (4), $\varepsilon = 1, 2, 3, 4$ and $5\,\mu$m, in the 3D setting. Figure 9 shows the dependence on A for the barrier height E_{sp} giving even splitting, the second reflection coefficient (R_2), the asymmetry parameter (7) and the radial oscillation amplitude (ρ_0). As expected, figure 9(a) shows that E_{sp} increases with increasing A. Under these conditions of strong nonlinearity ($N = 0.8N_c$), however, E_{sp} depends only weakly on the barrier width ε, with the exception of the narrowest barrier. Figure 9(b) shows that R_2 has the least sensitivity to A for the narrowest barrier with the required height being larger for smaller width, while R_2 is larger (as may be expected intuitively) for a larger width. An increase in A generally leads to only a weak modification of the asymmetry factor ζ, which is chiefly decreasing with A for wider barriers, presumably due to the larger speed of the soliton impinging upon the barrier, and correspondingly smaller interaction times. For narrow barriers, the dependence on A is more pronounced and non-monotonic. Figure 9(d) shows that transverse excitation is stronger for more energetic solitons and narrower barriers, where the interaction with the barrier is more impulsive. We expect transverse excitation to be more probable when the atomic kinetic energy is comparable with the transverse mode spacing $\hbar\omega_\perp$. This occurs when $A = 164\,\mu$m, which is reasonably consistent with the sudden increase in ρ_0 observed for $A \simeq 100\,\mu$m.

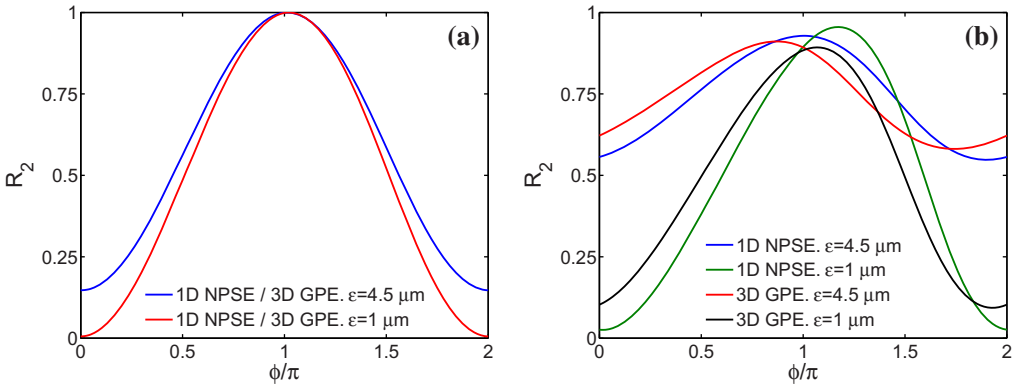

Figure 10. Second reflection coefficient, R_2, in the case of the initial 50% splitting, as a function of the phase difference introduced between the fragments at the time of their largest separation. The panels correspond to (a) $N \approx 0.06N_c$ (near the linear limit, shown for comparison) and (b) $N \approx 0.8N_c$. Notice that in the former case, the results for 1D and 3D settings coincide for $\varepsilon = 4.5\,\mu$m. In all cases, the initial displacement of the soliton was $A = 251\,\mu$m.

We note that the most significant, although small, differences between the quasi-1D setting of the NPSE and the full 3D setting arise in the case of narrow barriers. This is intuitively reasonable, as a narrow barrier induces dynamics on length scales closer to the transverse confinement and hence enhances the degree of transverse excitations, thus affecting the quality of the approximation of the 3D behavior by the quasi-1D NPSE. Nevertheless, between the two, there is still a reasonable qualitative agreement.

3.3. Effects of phase imprinting

Finally, we briefly analyze the effect of imprinting a phase difference at a certain time, $t = \pi/\omega_z$, onto the initially transmitted fragment, thereby emulating the operation of an interferometer. The phase difference is introduced when the fragments are located at the largest distance from the barrier. Figure 10 shows the second reflection coefficient, R_2, in the case of small (for comparison) and large atom numbers, as obtained from the simulations of the quasi-1D NPSE (1) and the 3D GPE (3). It is seen that, in the regimes of small N, the absence of a phase shift provides a nearly complete transmission, while a relative phase shift of π leads to almost perfect reflection. The contrast is considerably reduced for strong nonlinearity and sufficiently wide barriers, as shown in the right panel of figure 10, although a wider range of transmittivities/reflectivities is accessible for narrower barriers. In that light, although highly nonlinear waves (such as solitons) may be deemed less useful for interferometric purposes, their relevance may be (at least partially) restored in the context of suitably narrow barriers.

4. Conclusion

We have explored the collision of matter–wave solitons with a central barrier of variable width and height, inserted into a shallow harmonic-oscillator axial trap, and the subsequent collision

of the split fragments upon their return to the defect. This configuration forms the basis of a soliton interferometer. The non-monotonic variation of R_2 with N and E, evident for strong nonlinearity in figures 3 and 5, is detrimental to the sensitivity of an atom interferometer. Figure 10, however, indicates that the sensitivity to phase variation can be regained by smaller nonlinearity and that the adverse effect of strong nonlinearity can be partially mitigated by a narrow barrier. Narrow in this context evidently means in comparison to the axial size of the soliton.

Our analysis accounted for relatively large atom numbers, which are not much smaller than the collapse threshold. This strong nonlinearity necessitates a full 3D solution, in contrast to the 1D GPE setting studied in previous work. The analysis was carried out, in parallel, in the framework of the quasi-1D NPSE and the full 3D GPE, indicating good qualitative and even reasonable quantitative (at least not too close to $N = N_c$) agreement between the two. A detailed computational map of the ensuing phenomenology has been generated as a function of the number of atoms in the soliton, its initial distance from the barrier (which determines the collision velocity), and the height and width of the splitting barrier. Additionally, the effect of a phase shift imposed on the fragments at the moment of the largest separation was also examined.

A number of general conclusions, obtained in the framework of the quasi-1D and the full 3D settings, and their similarities and differences have been reported. While the results are similar between these two cases, they are essentially different from those generated by the 1D cubic GPE, which was used previously. The quasi-1D NPSE and the 3D GPE produce similar values for the first reflectivities, systematically increasing with increasing barrier height E and weakly decreasing with increasing number of atoms N. The second reflectivity (corresponding to the collision of the fragments after the first interaction with the barrier) oscillates strongly from complete reflection to high transmission as a function of the barrier height (and atom number). These oscillations are a fundamentally nonlinear effect, most pronounced for large N. The excitation of the transverse breathing mode was also characterized in the framework of the 3D GPE. This effect was found to become progressively more significant as the critical number of atoms, corresponding to the onset of the collapse, was approached. Phase imprinting was found to play a critical role in the outcome of the second collision, especially for small nonlinearity, modifying it between nearly complete transmission and full reflection. The highly nonlinear realm seems less sensitive to such variations, but the sensitivity may be restored for narrower barriers.

It is important to corroborate these findings experimentally. Regarding further theoretical analysis, a challenging problem is to study deviations of the results from the mean-field approximation in the 3D geometry as a function of the atom number N, in analogy to the recent studies in the 1D setting [27, 28, 31]. An additional issue of interest is the use of potential wells, rather than barriers, for which more complex phenomenology may be expected in the 3D setting [35, 36]. Lastly, extending such considerations to dark solitons in condensates with self-repulsive nonlinearity [41], and to multi-component systems [33, 42] are also compelling topics for further investigation.

Acknowledgments

This work was supported, in part, by grant no. 2010239 from the Binational (US–Israel) Science Foundation. JC acknowledges financial support from the MICINN project FIS2008-04848.

The work at Rice was supported by the NSF (PHY-1102515), ONR, the Norman Hackerman Advanced Research Program of Texas and the Welch Foundation (C-1133). PGK acknoweldges support from the US-NSF through grant DMS-0806762 and from the Alexander von Humboldt Foundation. We are indebted to Faustino Palmero for setting up the HPC cluster where the simulations were performed.

References

[1] Pethick C J and Smith H 2001 *Bose–Einstein Condensation in Dilute Gases* (Cambridge: Cambridge University Press)
[2] Pitaevskii L P and Stringari S 2003 *Bose–Einstein Condensation* (Oxford: Oxford University Press)
[3] Dalfovo F, Giorgini S, Pitaevskii L P and Stringari S 1999 *Rev. Mod. Phys.* **71** 463
[4] Kevrekidis P G, Frantzeskakis D J and Carretero-González R (ed) 2008 *Emergent Nonlinear Phenomena in Bose–Einstein Condensates Theory and Experiment* (Berlin: Springer)
[5] Hauke P, Cucchietti F M Tagliacozzo L, Deutsch I and Lewenstein M 2012 *Rep. Progr. Phys.* **75** 082401
[6] Strecker K E, Partridge G B, Truscott A G and Hulet R G 2003 *New J. Phys.* **5** 73
[7] Brazhnyi V A and Konotop V V 2004 *Mod. Phys. Lett.* B **18** 627–51
[8] Abdullaev F Kh, Gammal A, Kamchatnov A M and Tomio L 2005 *Int. J. Mod. Phys.* B **19** 3415
[9] Malomed B A, Mihalache D, Wise F and Torner L 2005 *J. Opt. B: Quantum Semicl. Opt.* **7** R53
[10] Morsch O and Oberthaler M 2006 *Rev. Mod. Phys.* **78** 179
Yurovsky V A, Olshani M and Weiss D S 2008 *Adv. At. Mol. Opt. Phys.* **55** 61
Lahaye T, Menotti C, Santos L, Lewenstein M and Pfau T 2009 *Rep. Progr. Phys.* **72** 126401
Kartashov Y V, Malomed B A and Torner L 2011 *Rev. Mod. Phys.* **83** 247
Kawaguchi Y and Ueda M 2012 *Phys. Rep.* **520** 253
[11] Frantzeskakis D J 2010 *J. Phys. A: Math. Theor.* **43** 213001
[12] Fetter A L and Svidzinsky A A 2001 *J. Phys.: Condens. Matter* **13** R135–94
[13] Kevrekidis P G, Carretero-González R, Frantzeskakis D J and Kevrekidis I G 2004 *Mod. Phys. Lett.* B **18** 1481–505
[14] Kasamatsu K, Tsubota M and Ueda M 2005 *Int. J. Mod. Phys.* B **19** 1835
[15] Fetter A L 2009 *Rev. Mod. Phys.* **81** 647–91
[16] Strecker K E, Partridge G B, Truscott A G and Hulet R G 2002 *Nature* **417** 150–3
[17] Cronin A D, Schmiedmayer J and Pritchard D E 2009 *Rev. Mod. Phys.* **81** 105
[18] Gustavsson M, Haller E, Mark M J, Danzl J G, Hart R, Daley A J and Nägerl H-C 2012 *New J. Phys.* **12** 065029
Grond J, Hohenester U, Mazets I and Schmiedmayer J 2012 *New J. Phys.* **12** 065036
Gross C, Zibold T, Nicklas E, Estève J and Oberthaler M K 2010 *Nature* **464** 1165
Tacla A B, Boixo S, Datta A, Shaji A and Caves C M 2010 *Phys. Rev.* A **82** 053636
Lücke B *et al* 2011 *Science* **334** 773
Grond J, Hohenester U, Schmiedmayer J and Smerzi A 2011 *Phys. Rev.* A **84** 023619
Jendrzejewski F, Müller K, Richard J, Date A, Plisson T, Bouyer P, Aspect A and Josse V 2012 *Phys. Rev. Lett.* **109** 195302
Rab M, Hayward A L C, Cole J H, Greentree A D and Martin A M 2012 *Phys. Rev.* A **86** 063605
[19] Geiger R *et al* 2011 *Nature Commun.* **2** 474
[20] See the presentation Kasevich M 2012 *NASA Quantum Future Technologies Conference* (17–21 January 2012) http://quantum.nasa.gov/agenda.html
[21] Veretenov N, Rozhdestvenskaya Yu, Rosanov N, Smirnov V and Fedorov S 2007 *Eur. Phys. J.* D **42** 455
[22] Khaykovich L, Schreck F, Ferrari G, Bourdel T, Cubizolles J, Carr L D, Castin Y and Salomon C 2002 *Science* **296** 1290–3
[23] Cornish S L, Thompson S T and Wieman C E 2006 *Phys. Rev. Lett.* **96** 170401

[24] Eiermann B, Anker B Th, Albiez M, Taglieber M, Treutlein P, Marzlin K-P and Oberthaler M K 2004 *Phys. Rev. Lett.* **92** 230401
[25] Ilo-Okeke E O and Zozulya A A 2010 *Phys. Rev.* A **82** 053603
London U and Gat O 2011 *Phys. Rev.* A **84** 063613
Fujishima H, Mine M, Okumura M and Yajima T 2011 *J. Phys. Soc. Japan* **80** 084003
Billam T P, Cornish S L and Gardiner S A 2011 *Phys. Rev.* A **83** 041602
Carr L D, Miller R R, Bolton D R and Strong S A 2012 *Phys. Rev.* A **86** 023621
Abdullaev F Kh and Brazhnyi V A 2012 *J. Phys. B: At. Mol. Opt. Phys.* **45** 085301
Gertjerenken B and Weiss C 2012 *J. Phys. B: At. Mol. Opt. Phys.* **45** 165301
[26] Helm J L, Billam T P and Gardiner S A 2012 *Phys. Rev.* A **85** 053621
[27] Martin A D and Ruostekoski J 2012 *New J. Phys.* **14** 043040
[28] Gertjerenken B, Billam T P, Khaykovich L and Weiss C 2012 *Phys. Rev.* A **86** 033608
[29] Billam T P, Marchant A L, Cornish S L, Gardiner S A and Parker N G 2013 Bright solitary matter waves: formation, stability and interactions *Spontaneous Symmetry Breaking, Self-Trapping, and Josephson Oscillations* (*Progress in Optical Science and Photonics* vol 1) ed B A Malomed (Berlin: Springer)
[30] Parker N G, Martin A M, Cornish S L and Adams C S 2008 *J. Phys. B: At. Mol. Opt. Phys.* **41** 045303
[31] Weiss C and Castin Y 2012 *J. Phys. A: Math. Theor.* **45** 455306
[32] Wang C-H, Homg T-M, Lee R-K and Wang D-W 2012 *Opt. Exp.* **20** 22675
[33] Hansen S D, Nygaard N and Mølmer K 2012 Scattering of matter wave solitons on localized potentials arXiv:1210.1681
[34] Holmer J, Marzuola J and Zworski M 2007 *Commun. Math. Phys.* **274** 187
Holmer J, Marzuola J and Zworski M 2007 *J. Nonlin. Sci.* **17** 349
[35] Lee C and Brand J 2006 *Europhys. Lett.* **73** 321
[36] Ernst T and Brand J 2010 *Phys. Rev.* A **81** 033614
[37] Salasnich L, Parola A and Reatto L 2002 *Phys. Rev.* A **65** 043614
[38] Salasnich L, Malomed B A and Toigo F 2007 *Phys. Rev.* A **76** 063614
Salasnich L, Malomed B A and Toigo F 2008 *Phys. Rev.* A **77** 035601
[39] Sulem C and Sulem P L 1999 *The Nonlinear Schrödinger Equation* (New York: Springer)
[40] Bergé L 1998 *Phys. Rep.* **303** 259
Kuznetsov E A and Dias F 2011 *Phys. Rep.* **507** 43
[41] Frantzeskakis D J, Theocharis G, Diakonos F K, Schmelcher P and Kivshar Yu S 2002 *Phys. Rev.* A **66** 053608
[42] Álvarez A, Cuevas J, Romero F R, Hamner C, Chang J J, Engels P, Kevrekidis P G and Frantzeskakis D J 2013 *J. Phys. B: At. Mol. Opt. Phys.* **46** 065302